COMBINED SIMULATION AND INVERSION OF SP AND RESISTIVITY LOGS FOR THE ESTIMATION OF CONNATE WATER RESISTIVITY AND ARCHIE'S CEMENTATION EXPONENT

Jesús M. Salazar, Gong Li Wang, Carlos Torres-Verdín, and Hee Jae Lee, The University of Texas at Austin

This paper was prepared for presentation at the SPWLA 48th Annual Logging Symposium held in Austin, Texas, United States, June 3-6, 2007.

ABSTRACT

Knowledge of initial water saturation is vital to estimate original oil in place. In addition, accurate estimation of permeability is necessary to select perforation intervals, layers for fluid injection, and to forecast production. Reliable assessment of these two petrophysical properties is possible when rock-core measurements are available. However, such measurements are not always available, and if they are, their reliability is sometimes questionable.

This paper describes a new inversion methodology to estimate connate water resistivity (R_w) and Archie's cementation exponent (*m),* from the combined use of borehole raw array-induction resistivity measurements and spontaneous potential (SP) in water-bearing intervals. Combined inversion of resistivity and SP measurements is performed assuming a piston-like invasion profile. In so doing, the reservoir is divided into petrophysical layers to account for vertical heterogeneities. Inversion products are values of invaded and virgin formation resistivity, radius of invasion, and static spontaneous potential (*SSP*). Connate water resistivity is calculated by assuming membrane and diffusion potentials as the main contributors to the *SSP*. Archie's or dual-water equations enable the estimation of *m*.

We successfully applied this combined estimation method to two data sets acquired in clastic formations. One data set corresponds to a high-permeability, low-salt concentration reservoir and the second set is associated with a high-permeability, high-salt concentration formation. Values of R_w and *m* yielded by the inversion are consistent with those obtained from Pickett's plots, thereby confirming the reliability of the estimation. Results are used as input to estimate water saturation in hydrocarbon-bearing intervals. Accurate estimation of initial water saturation allows us to apply the physics of mud-filtrate invasion to estimate permeability. By progressively modifying permeability and performing multiple mud-filtrate invasion simulations we are able to match borehole resistivity measurements, thereby obtaining the estimate of absolute permeability. In a vertically heterogeneous formation, the estimated permeability increases between 25% and 85% with respect to the initial-guess in the most prospective intervals. The method described in this paper is an efficient alternative to perform petrophysical analysis of exploratory and appraisal wells wherein rock-core measurements may not be available.

H

INTRODUCTION

Initial water saturation in a hydrocarbon reservoir has an enormous impact on the calculation and production of original oil in place. In addition, permeability is regarded as the most important variable in selecting perforation intervals, layers for injection, and to forecast production. When laboratory measurements (core, water analysis, etc.) are available, these two variables are properly constrained. However, such measurements are not always available, and if they are, their reliability may be questionable. Therefore, there is a strong need for alternative methods to estimate initial water saturation and permeability.

Two of the main parameters needed to calculate water saturation are R_w and *m*, which can be obtained from connate water analysis and special core analysis, respectively. Core measurements are often expensive because they involve the cost of extracting the core sample and laboratory work. Moreover, measurements of water resistivity are difficult due to the need to acquire connate water samples when wells are already in production and water-injection/steam-flood have been applied to enhance production. Fluid samples taken by fluid acquisition tools are often contaminated with mud-filtrate and/or hydrocarbon.

In the early days of formation evaluation, SP and resistivity measurements were the only borehole measurements available for interpretation to log analysts or petrophysicists (Doll, 1949). Today, with the introduction of modern logging tools, young professionals pay little attention to SP. One of the first physical models of SP was developed using a resistor network (Segesman, 1962), where dipole layers were simulated using voltage sources. Zhang and Wang

(1997 and 1999) developed a finite-element algorithm to simulate SP measurements using the vector and scalar potential theory. Their algorithm successfully reproduced the resistor model developed by Segesman. In this paper, we simulate SP measurements using Zhang and Wang's algorithm. Our main objective is to use SP measurements to calculate R_w and m based on the combined inversion of raw AIT[1] and SP measurements. Values of R_w obtained with this method are compared to those obtained with Pickett's plots (Pickett, 1966).

We use two different data sets acquired in clastic formations to test the estimation method developed in this paper. In one case, raw measurements are available to perform the analysis in a water-bearing interval. The second well displays a down-dip interval below a possible water-oil-contact and was logged using dual laterolog (DLL). The University of Texas Formation Evaluation Toolbox (UTFET) is used to model DLL and to infer the spatial distribution of electrical resistivity in the invaded formation. From this distribution, we simulate raw AIT measurements. Finally, we compare the value of m obtained from core measurements in the second well to that estimated with the combined inversion of SP and resistivity measurements.

RESISTIVITY MODELING AND INVERSION

The purpose of resistivity modeling and inversion is to estimate the invaded zone (R_{xo}) and virgin zone (R_t) resistivities and the radius of invasion (r_{inv}) from raw array-induction conductivity measurements. Figure 1 shows the earth model assumed in the simulations. Initially, we assume a single-layer case and a piston-like radial profile of invasion. The system is bounded at the top and bottom by shale beds (shoulders) with resistivity R_{shtop} and R_{shbot}, respectively. Also, the model is bounded by a borehole with fluid resistivity equal to R_m and the virgin zone whose resistivity is one of the main inputs necessary to estimate water saturation.

An induction tool measures formation resistivity by inducing low-frequency electric currents into the formation surrounding the borehole. The simulation of induction measurements assumes a 2D axial-symmetric model where current loop sources are located at the center of the borehole. We use the Numerical-Mode Matching Method (NMM) to perform the corresponding simulations (Chew et al., 1984; Zhang et al., 1999). On the other hand, the inverse problem of raw array-induction measurements is approached with the distorted Born iterative method (DBIM) (Chew and Liu, 1994). Appendix A describes the process of modeling and inversion of array-induction resistivity measurements.

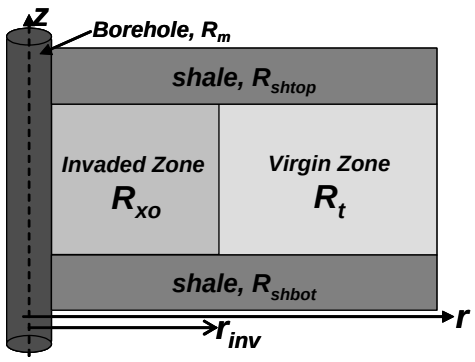

Figure 1: Single layer earth model assumed in the simulation and inversion of borehole resistivity measurements. The model assumes a piston-like invasion front.

MODEL OF SPONTANEOUS POTENTIAL

The SP has four main components (Hallemburg, 1971): the diffusion potential, the membrane or Nernst potential (known as the electrochemical components), the electro-kinetic or streaming potential, and the oxidation/reduction phenomenon (redox). Electro-kinetic and redox components are negligible in borehole applications compared to the electrochemical components. In this paper, we focus our work exclusively to the diffusion and membrane potentials.

The total potential measured by a borehole SP tool is primarily the algebraic sum of the membrane and diffusion potential components (Wyllie and Southwick, 1954). In a permeable zone at borehole conditions, the maximum potential (in absolute value) is known as the static SP (*SSP*). The *SSP* at borehole conditions is measured with respect to a shale baseline (Pirson, 1963) and in mV units is given by

$$SSP \cong -70.7 \cdot \left(\frac{460 + T_F}{537} \right) \log \left(\frac{R_{mfe}}{R_{we}} \right), \qquad (1)$$

where R_{we} designates the equivalent water resistivity, R_{mfe} is the equivalent mud-filtrate resistivity, and T_F is the formation temperature in ^{o}F. We use equation (1) to estimate R_w via the combined inversion of SP and resistivity measurements.

Modeling and Inversion: In the forward model, electrochemical components are considered as the only contributors to the *SSP*. The *SSP* is basically an

[1] Mark of Schlumberger

electromotive force due to electric dipole layers distributed along the borehole wall, invasion fronts, and formation boundaries. In this study, vector potential theory (Zhang and Wang, 1997 and 1999) is used to compute SP in a water-base mud-filled borehole. Accordingly, electric dipole layers that could extend to infinity are replaced by magnetic current rings located at the intersection points of the borehole wall, invasion fronts, and formation boundaries. In cylindrical coordinates (r,z), the governing equation is given by

$$\frac{1}{2\pi}\left[\frac{\partial}{\partial r}\frac{R}{r}\frac{\partial}{\partial r}+\frac{\partial}{\partial z}\frac{R}{r}\frac{\partial}{\partial z}\right]V=-\varepsilon_{SSP}\delta\left(r-r_s\right)\delta\left(z-z_s\right),$$

where V is the electric potential, R the electrical resistivity of the formation, and r_s and z_s the radial and vertical position of a source in the meridian plane representing a magnetic current ring in 3D space. We use the 2D finite-element method to solve this problem with a front solver to expedite the solution of the resulting linear system of equations.

Results from resistivity inversion are used as the main input to the inversion of SP measurements. The algorithm also considers mud resistivity, borehole radius, and layer boundary positions for both resistivity and SP inversion. Inversion of SP to obtain *SSP* from field data is posed as a linear problem and solved using the singular value decomposition (SVD) method. Figure 2 shows a multi-layer earth model (heterogeneous formation) assuming three invaded layers with different radii of invasion and resistivities for each cylindrical and vertical layer. The resistivity at each block (R_{xo} and R_t) and the *SSP* at each layer boundary are the final results obtained with the combined inversion of SP and resistivity measurements.

ESTIMATION OF R_w AND m

Field SP data, AIT raw measurements, borehole, and mud data are used as inputs for the combined SP-Resistivity inversion. Resistivity inverted results are input for SP inversion. In order to estimate connate water resistivity, the inversion is carried out in a wet sand interval. Once the *SSP* is obtained at each layer boundary from the inverted SP, the equivalent water resistivity is computed with the maximum negative *SSP* via equation (1). Subsequently, an empirical correlation from log interpretation charts (Schlumberger, 1991; Bigelow, 1992) is used to estimate R_w, namely,

$$R_w=\frac{R_{we}+0.131\cdot 10^{\left[\frac{1}{\log(T_F/19.9)}-2\right]}}{-0.5\cdot R_{we}+10^{\left[\frac{0.0426}{\log(T_F/50.8)}\right]}}. \qquad (2)$$

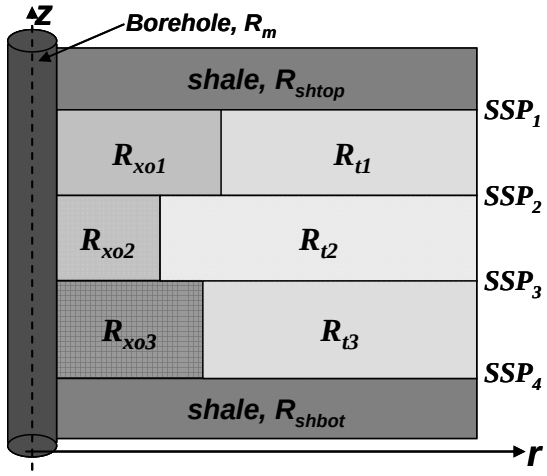

Figure 2: Multi-layer earth model assumed in the combined simulation and inversion of resistivity and SP measurements.

In our method we assume the formation water as a solution of NaCl. Therefore, equation (2) is not valid for all types of formation water or waters with high salt concentration (above 220 kppm). Additional transformations need to be applied for the case of water with components other than NaCl (Bigelow, 1992).

For the estimation of the cementation exponent, we initially assume a clean (shale-free) 100% water saturated clastic sequence. Archie's equation (Archie, 1942) is used to compute the cementation exponent without specific adjustments for presence of shale, as follows:

$$m=\frac{1}{\log(\phi)}\log\left(\frac{a\cdot R_w}{R_t}\right), \qquad (3)$$

where a is the tortuosity factor and ϕ is the inter-connected porosity taken as an average in the interval of analysis. On the other hand, when shaliness is considered, we use the dual-water model for shaly sands (Clavier et al., 1984) since several of its governing parameters can be calculated from well logs (Dewan, 1983), namely,

$$m=\frac{1}{\log(\phi)}\log\left(\frac{a\cdot R_w}{R_t}\left[1-S_b\left(1-\frac{R_w}{R_b}\right)\right]^{-1}\right), \qquad (4)$$

where S_b and R_b are bound water saturation and bound water resistivity, respectively. Equation (4) is valid in wet sands and reduces to equation (3) in clean sands (where $S_b = 0$). Figure 3 is a flow diagram that summarizes the steps used to estimate connate water resistivity and cementation exponent via the combined inversion of resistivity and SP measurements.

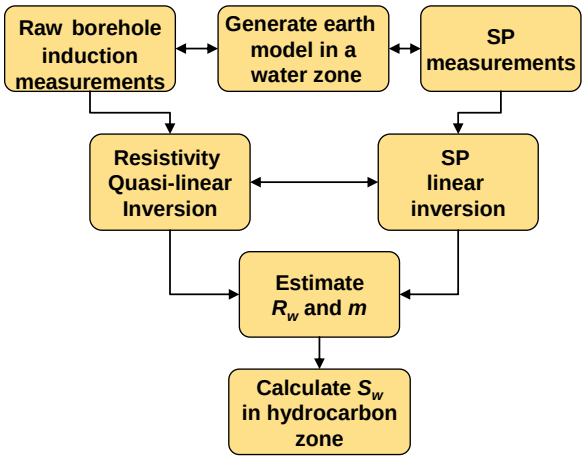

Figure 3: Flow chart describing the algorithmic steps followed for the combined simulation and inversion of resistivity and SP measurements to estimate R_w and m, and to calculate water saturation in hydrocarbon zones.

FIELD CASES OF STUDY

The cases under analysis correspond to fairly clean clastic formations from different locations of the world. Both rock formations are 100% water-saturated, with Formation No. 1 (hereafter referred to as F-1) having high salt concentration (>100 kppm) whereas Formation No. 2 (hereafter referred to as F-2) has a low salinity (<15 kppm). Table 1 is a summary of the thickness and average petrophysical properties of each formation. Figures 4 and 5 display the well logs and estimated porosity and permeability for F-1 and F-2, respectively. Well logs include gamma ray (GR), SP, and AIT resistivity (2-foot vertical resolution) for F-1 and Dual Laterolog (LLS, LLD) and MSFL[2] (Microespherically Focused Log) for F-2. Porosity is computed from density-neutron logs via a non-linear dual-mineral (shale-quartz) model and permeability from a modified Timur-Tixier equation (Balan et al., 1995). Water saturation (S_w) is not shown here since both formations are completely water-saturated (S_w=*100%*).

***Combined Inversion*:** In Formation No. 2, AIT resistivity measurements were not available. Therefore, we use the physics of mud-filtrate invasion to reproduce the spatial distribution of electrical resistivity (Salazar et al., 2006) in the interval of analysis. As a result of the simulation of mud-filtrate invasion, we obtained spatial distributions of water saturation, salt concentration (Figure 6), and electrical resistivity (Figure 7) via Archie's equation at a desired time frame. Finally, AIT measurements were modeled using the spatial distribution of electrical resistivity with the Numerical-Mode Matching Method (Zhang et al., 1999). Only raw AIT modeled data were used to perform the combined inversion of SP and resistivity measurements.

To proceed with the combined Resistivity-SP inversion, Formation No. 1 is divided into three petrophysical layers, whereas Formation No. 2 is divided in two petrophysical layers or flow sub-units. Layer selection is based upon main resistivity changes and petrophysical properties (porosity-permeability). For resistivity inversion, inputs are layer boundaries, borehole radius and conductivity, and raw AIT conductivity data. Inversion results are values of R_{xo}, R_t, and r_{inv} for each layer, which are additional inputs to the SP inversion. Once the inversion is finished, we obtain values of *SSP* at each layer boundary. Table 2 and Table 3 describe the inversion results for Formation No. 1 and Formation No. 2, respectively. Figures 8 and 9 show the results of resistivity inversion together with the SP simulation for each formation.

Table 1- Summary of average petrophysical properties assumed for the two case studies.

Property	Units	F-1	F- 2
Thickness	ft	58	36
Effective porosity	fraction	0.30	0.17
Water saturation	fraction	1.0	1.0
Shale concentration	fraction	0.02-0.10	0.05-0.15
Permeability	md	100-2000	1000-2500

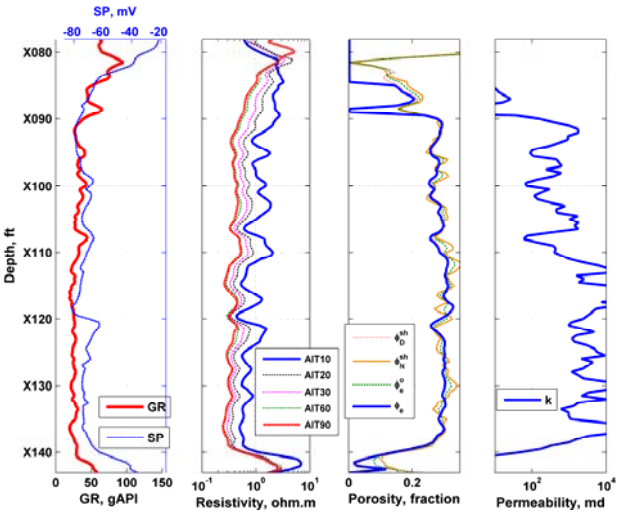

Figure 4: Well logs and petrophysical properties for Formation No. 1. Separation of AIT resistivity curves indicates invasion of mud filtrate into the wet sand. The porosity track shows shale-corrected density and neutron porosity (ϕ_D^{sh} and ϕ_N^{sh}), effective initial-guess porosity (ϕ_e^o), and effective porosity obtained with a nonlinear model (ϕ_e).

[2] Mark of Schlumberger

Table 2- Inversion results for Formation No. 1

Thickness	R_{xo}	R_t	r_{inv}	*SSP*
ft	Ohm.m	Ohm.m	ft	mV
shoulder	3.7586	3.7586	0	56.4128
12	1.8938	0.5425	1.1519	-6.5244
19	1.1665	0.4849	1.2395	-1.7396
27	1.0916	0.3387	1.7618	-49.3705
shoulder	4.2012	4.2012	0	-

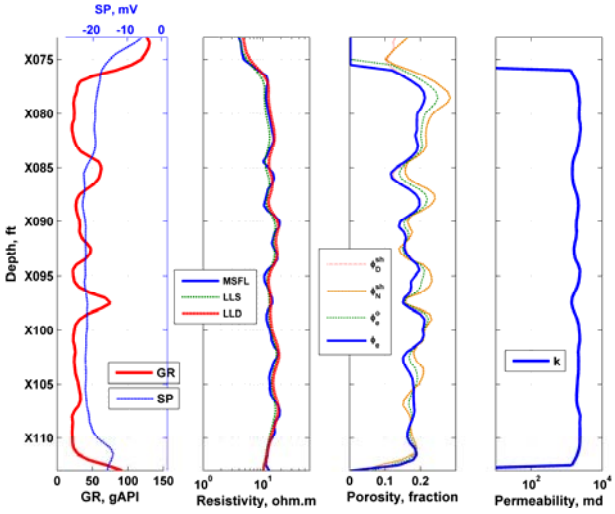

Figure 5: Well logs and petrophysical properties for Formation No. 2. This depth interval does not indicate deep invasion. The porosity track shows shale-corrected density and neutron porosity (ϕ_D^{sh} and ϕ_N^{sh}), effective initial-guess porosity (ϕ_e^o), and effective porosity (ϕ_e).

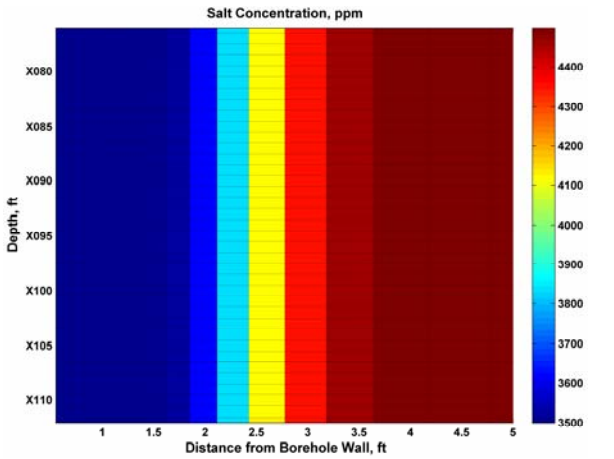

Figure 6: Spatial distribution of salt concentration for Formation No. 2 used to calculate electrical resistivity (after 2 days of invasion). Water saturation in this region is 100% (constant).

Table 3- Inversion results for Formation No. 2

Thickness	R_{xo}	R_t	r_{inv}	*SSP*
ft	Ohm.m	Ohm.m	ft	mV
shoulder	3.9790	3.9790	0	2.5070
8	48.0185	12.6596	0.7287	3.7139
28	28.6036	11.9738	1.0023	-23.3250
shoulder	10.7925	10.7925	0	-

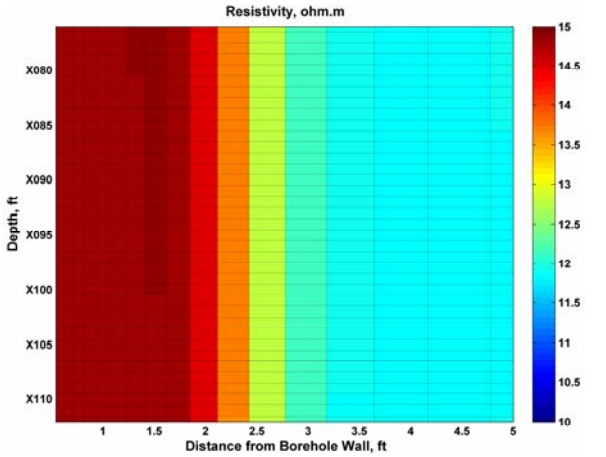

Figure 7: Spatial distribution of electrical resistivity for Formation No. 2 used to model AIT resistivity measurements (after 2 days of invasion). Electrical resistivity is calculated via Archie's equation assuming constant water saturation and variable salt concentration.

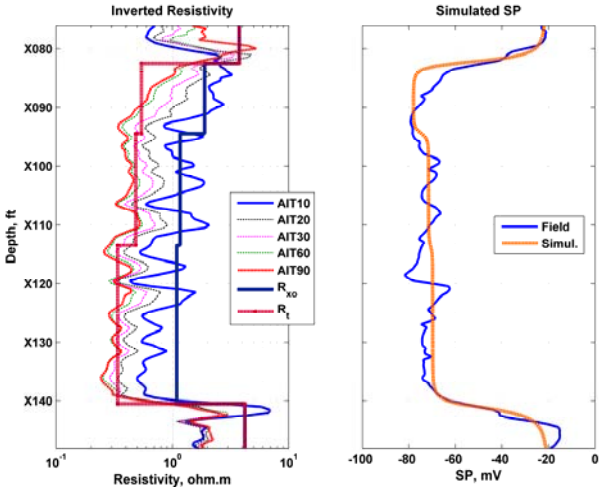

Figure 8: Results of the combined inversion of resistivity and SP for Formation No. 1. The right-hand panel compares inverted R_{xo} and R_t with field AIT (2-foot vertical resolution) measurements and the left-hand panel compares the simulated SP obtained to the inverted *SSP* from field SP measurements.

Assessment of m and R_w: Equivalent water resistivity is obtained from the inverted *SSP* via equation 1. Subsequently, connate water resistivity is computed at reservoir temperature using equation 2. Archie's (equation 3, for clean sands) and Dual-Water (equation

4, shaly-sands) models yield *m* using the new R_w and R_t obtained from inversion and porosity from logs. Table 4 describes the inverted values of R_w and *m*.

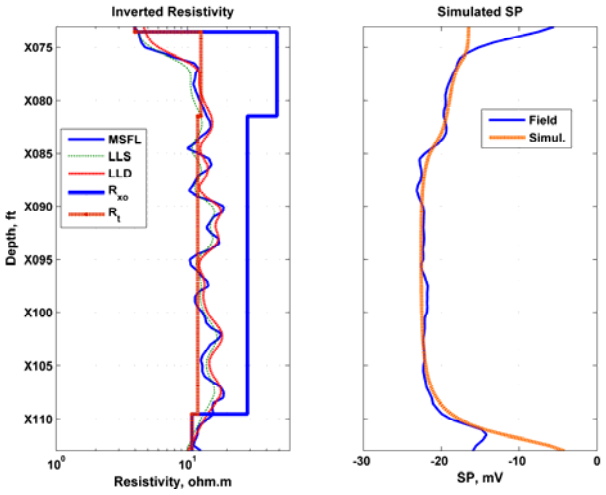

Figure 9: Results of the combined inversion of resistivity and SP for Formation No. 2. The right-hand panel compares inverted R_{xo} and R_t to field dual-laterolog measurements and the left-hand panel compares the simulated SP obtained to the inverted *SSP* from field SP measurements.

Table 4- Calculated values of connate water resistivity and cementation exponent.

Property	Units	F-1	F- 2
R_w	ohm.m	0.042	0.272
Temperature	°F	142	149
[NaCl]	ppm	105,000	11,000
m - Archie	-	1.74	2.14
m – Dual-Water	-	1.69	2.21
C_{sh}	%	10	10

When comparing the values of *m* obtained with Archie's equation to the one obtained with the Dual-Water equation we see a reduction in the cementation exponent on Formation No. 1. On the other hand, in Formation No. 2, shaliness causes the cementation exponent to increase. These opposite results are probably due to the high salt concentration (*[NaCl]*) in Formation No. 1 (above 100 kppm) compared to that of Formation No. 2 (below 11 kppm). Such different salinities make the true formation resistivity for each case to be two orders of magnitude different from each other. In Formation No. 2, three laboratory measurements of core formation factor were available that display an average *m = 1.60* for a *4,000 ppm* brine. By comparison, results for Formation No. 2 indicate a connate water salt concentration of *11,000 ppm*.

Appraisal of R_w: In order to cross-validate the results of connate water resistivity we built a traditional Pickett plot (Pickett, 1966). Figure 10 displays the corresponding Pickett plot for each formation. Values of R_w obtained from the Pickett plot were 0.037 ohm.m at 142 °F for F-1 and 0.3 ohm.m at 149 °F for F- 2. Such results represent a difference of 12% and 10% with respect to the values obtained from inversion for F-1 and F-2, respectively. The relatively small difference between the Pickett plot calculation and the inversion results lends credence to the reliability of the inversion method developed in this paper.

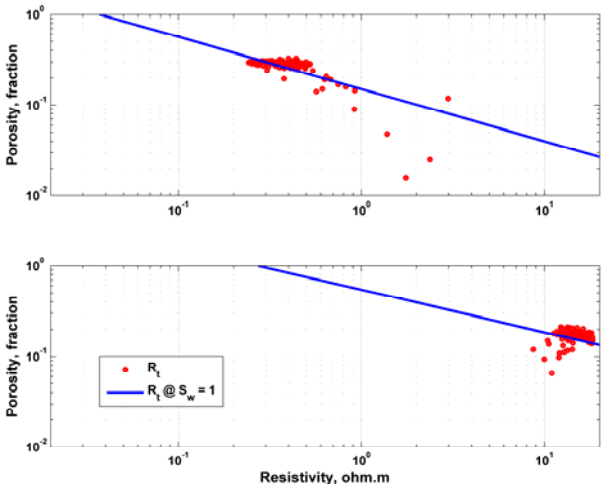

Figure 10: Pickett plot used to cross-validate the calculations of connate water resistivity. The top and bottom panels display results for Formation No. 1 and for Formation No. 2, respectively.

ASSESSMENT OF WATER SATURATION AND PERMEABILITY

Formation No. 3 (hereafter referred to as F-3) is the zone of interest for this analysis, which corresponds to a deeper interval of the well penetrating Formation No. 1. The well penetrates a North Louisiana tight-gas sand formation subject to water-base mud-filtrate invasion. Ideally, in a formation penetrating a water zone, we would directly use the results of the inversion (R_w and *m*) to estimate water saturation in the upper hydrocarbon zone. However, the geological characteristics of F-3 are different from those of F-1. Therefore, parameters used to calculate water saturation are slightly different for F-1. Table 5 shows the values used in the assessment of water saturation. The methodology, parameters, and simulation approach used to compute water saturation, porosity, initial guess of permeability, and permeability from resistivity matching, are described by Salazar et al. (2006).

Table 5- Summary of Archie's parameters and rock and fluid properties used to estimate water saturation and porosity (Salazar et al., 2006).

Variable	Units	Value
Archie's tortuosity factor *a*	-	1.00
Archie's cementation exponent *m*	-	1.95
Archie's saturation exponent *n*	-	1.75
Connate water resistivity @ 210 °F	ohm.m	0.02
Invasion water resistiv. @ 210 °F	ohm.m	0.56
Matrix density	g/cm^3	2.65
Shale density	g/cm^3	2.68
Water density	g/cm^3	1.00
Water-hydrocarbon density (mix.)	g/cm^3	0.50

Standard Petrophysical Assessment: F-3 consists of a fairly clean clastic sequence with high salt concentration (160 kppm). Therefore, we use Archie's equation without any further shale correction to calculate initial water saturation. Porosity is calculated with a non-linear dual-fluid dual-mineral equation that considers shale-corrected bulk density and neutron measurements. The initial guess of permeability is calculated with a modified Timur-Tixier equation. Figure 11 shows results of the petrophysical assessment, including porosity, initial water saturation, and permeability.

Permeability Assessment via the Simulation of Mud-Filtrate Invasion: Either resistivity matching or inversion (Salazar et al., 2005; Salazar et al., 2006) using the physics of mud-filtrate invasion are alternative methods for estimating permeability. In this paper, we use the method of manual resistivity matching which does not require the use of numerical inversion.

For the purpose of manual resistivity matching, we simulate the process of two-phase flow of water-base mud filtrate invading a partially gas-saturated formation. This problem is modeled as convective transport of aqueous and hydrocarbon phases, and components of water, hydrocarbon, and salt concentration (Alpak et al., 2003; Wu et al., 2005). Upper, lower, and external boundaries of the formation enforce no-flow conditions. We also account for the effect of capillary pressure and relative permeability as well as gravity effects in the mixing region. Modeling of multi-phase and multi-component fluid-flow is performed with The University of Texas' Formation Evaluation Toolbox (UTFET) which is a finite-difference, axial-symmetric reservoir simulator developed specifically for the simulation of mud-filtrate invasion. In the first stage of the simulation, a constant flow rate, obtained as the time average of the flow rate yielded by the FET, is imposed at the borehole wall for each numerical layer as a fixed source condition. Based on field reports, the zone under analysis was exposed between 3-5 days to mud-filtrate invasion. We calculate our results assuming 4 days of invasion. Table 6 describes the main mud parameters used to simulate the process of mud-filtrate invasion. The main outputs of the simulation are the spatial distributions of water saturation and salt concentration, which are used to calculate electrical resistivity via Archie's equation.

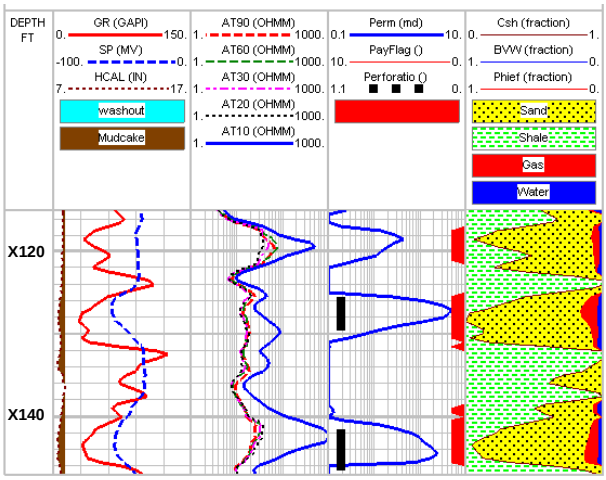

Figure 11: Petrophysical assessment of a clastic formation. Track 1 shows depth. Track 2 displays gamma-ray, SP and caliper. Track 3 shows the AIT resistivity measurements. Track 4 displays the initial-guess of permeability, pay thickness, and the location of perforations. Track 5 describes the volumetric analysis with shale concentration, bulk volume water, and effective porosity.

Table 6- Summary of mudcake, fluid, and formation properties assumed in the simulation of the process of mud-filtrate invasion.

Variable	Units	Value
Mudcake reference permeability	md	0.03
Mudcake reference porosity	fraction	0.30
Mud Solid Fraction	fraction	0.06
Mudcake maximum thickness	in	0.4
Mudcake compressibility exponent	fraction	0.40
Mudcake exponent multiplier	fraction	0.10
Mud hydrostatic pressure	psi	5,050
Initial formation pressure	psi	4,800
Mud-filtrate viscosity	cp	1.00
Gas viscosity	cp	0.02
Mud-filtrate density	lb/ft^3	62.4
Gas density	lb/ft^3	0.1
Salt concentration of mud-filtrate	ppm	3,000
Salt concentration of connate water	ppm	160,000
Wellbore radius	ft	0.35
Maximum invasion time	days	4.00
Temperature	°F	220
Formation outer boundary	ft	860
Residual water saturation	fraction	0.15
Residual gas saturation	fraction	0.10

Table 7- Summary of average petrophysical properties assumed for the case of a multi-layer formation.

Thickness, ft	*ϕ, frac.*	*S_w, frac.*	*k^o, md*
5.78	0.041	0.284	0.564
1.74	0.062	0.850	0.200
2.30	0.039	0.628	0.688
1.81	0.121	0.184	5.550
3.76	0.066	0.324	1.191
2.99	0.032	0.899	0.200
3.34	0.045	0.849	0.200
2.23	0.039	0.719	0.200
5.08	0.059	0.282	2.135

The next stage is the modeling of array-induction measurements from the spatial distribution of electrical resistivity. We use the numerical mode-matching method to approach this task. The fluid-flow simulator is coupled to the resistivity modeling code via a user-friendly interface. At the end of resistivity modeling, field AIT resistivity measurements are compared to those obtained from the simulation. If there is no agreement between the two data sets, we modify the permeability of each petrophysical layer and perform the simulation again. This process is repeated several times until reaching an acceptable match between field and simulated resistivity.

In order to account for vertical heterogeneities in the formation under analysis, we subdivided F-3 into nine flow sub-units (horizontal layers). Such subdivision was based on observed permeability-porosity and resistivity changes. Table 7 describes average petrophysical properties such as porosity, initial water saturation, and initial estimate of permeability obtained from the petrophysical assessment. These properties are considered constant in the radial direction away from the wellbore for each flow sub unit. By dividing the reservoir into several layers, we honor the fact that capillary pressure and other petrophysical properties are specific to each layer. Accordingly, the flow rate of mud-filtrate invasion is also different for each flow sub unit.

Figure 12 shows the results of the simulation of the process of mud-filtrate invasion after the initial permeability of each layer was modified to match the array-induction resistivity measurements. Figure 13 shows 2-foot vertical resolution AIT curves simulated before and after manually changing the values of layer permeability, as well as a comparison between initial-guess and matching permeability. Figure 14 compares simulated and field AIT measurements (2-foot vertical resolution). We observe a good match for R60 and R90 curves and a fair match for the R10, R20, and R30 curves. The presence of a resistivity annulus and deep

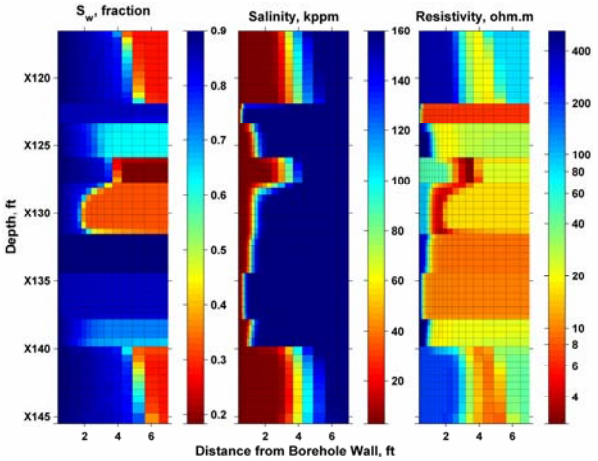

Figure 12: Spatial distributions of water saturation, salt concentration, and electrical resistivity for Formation No. 3 after four days of mud-filtrate invasion. The spatial distribution was calculated after permeability was adjusted multiple times to fit the available array-induction resistivity measurements.

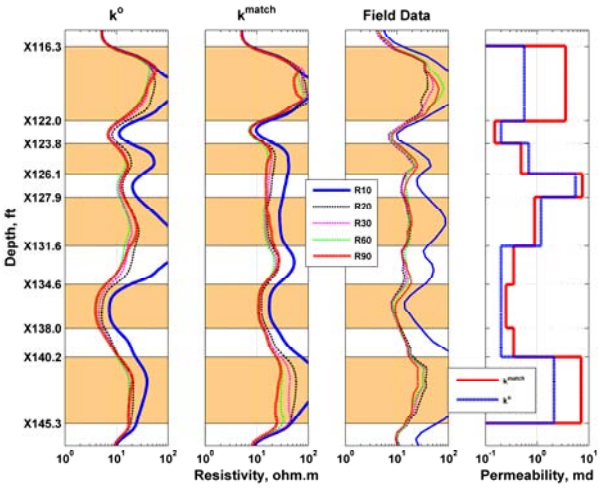

Figure 13: Two-foot vertical resolution array-induction resistivity measurements before (Track 1) and after (Track 2) resistivity matching by manually changing the permeability. The right-most tracks show field resistivity data as well as a comparison between the initial guess and matching values of permeability. Shaded rectangles identify the various layers assumed in the simulation.

invasion makes the matching even more challenging as one can observe in the upper-most and lower-most layers of the formation.

Based on this analysis, we note that permeability calculated from a modified Timur-Tixier equation is underestimated in the most prospective zones of the formation. The new permeability obtained via resistivity matching is between 25% and 85% larger than the initial-guess permeability obtained with a conventional Timur-Tixier model. Permeability values

obtained with the method of resistivity matching are in the same order of magnitude as those measured from rock-core samples acquired in a nearby field penetrating the same formation (Luffel et al., 1991).

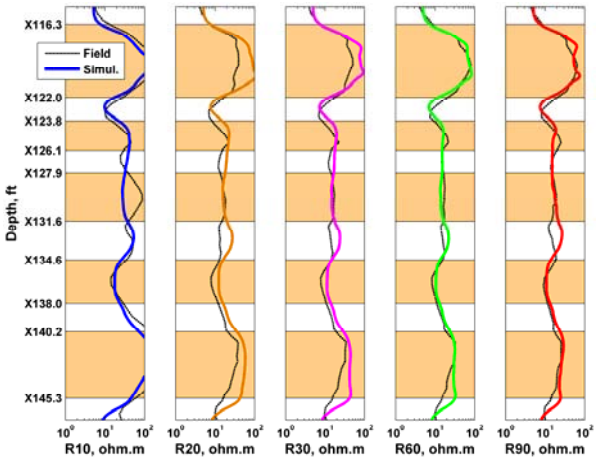

Figure 14: Comparison of field and simulated array-induction resistivity curves after resistivity matching for five radial lengths of investigation. The match was secured after five manual modifications of layer permeability. Continuous thick curves identify simulated values and thin dashed curves identify field data.

CONCLUSIONS

The combined inversion of resistivity and SP measurements is a reliable method to estimate R_w and m in wet formations. Results obtained from the inversion were consistent with those obtained from Pickett's plots. The difference between the estimates obtained with the two methods was of the order of 10%. When shaliness was considered in the estimation of m, results also showed dependence on salt concentration, yielding higher values of m in low-salinity formations and lower values of m in high-salinity formations.

The values obtained from inversion provided a starting point to accurately estimate water saturation and layer-by-layer permeability via resistivity matching. In general, the calculated values of layer permeability were approximately 25%-85% higher than those of the initial-guess permeability. The combined inversion method is highly recommended in zones where NaCl is the most abundant salt component and where connate salt concentration does not change in short depth intervals. This method of inversion works very well in high-permeability thick formations and connate water with high salt concentration.

In zones where the most abundant salt components are different from NaCl (e.g., $CaCl_2$, KCl, etc.) equation (1) is not valid. In addition, when the salt concentration of mud-filtrate and connate water are similar, the deflection of the SP curve is marginal, and therefore, the inversion method is not recommended. In low-permeability (< 5 md) formations the electrokinetic components of the SP may become important for the total contribution to *SSP* and may need to be considered before applying the inversion method explained in this paper.

In the absence of water zones, resistivity inversion can still be used to obtain R_{xo} and R_t for an accurate calculation of initial water saturation. This calculation method can be useful in the petrophysical assessment of exploratory and appraisal wells that are normally devoid of core and laboratory measurements.

H

ACKNOWLEDGEMENTS

We are obliged to ConocoPhillips and Occidental Petroleum Corporation for permission to publish field results. The work reported in this paper was funded by the University of Texas at Austin's Research Consortium on Formation Evaluation, jointly sponsored by Anadarko, Aramco, Baker Atlas, BP, British Gas, ConocoPhillips, Chevron, ENI E&P, ExxonMobil, Halliburton Energy Services, Hydro, Marathon Oil Corporation, Mexican Institute for Petroleum, Occidental Petroleum Corporation, Petrobras, Schlumberger, Shell International E&P, Statoil, TOTAL, and Weatherford.

REFERENCES

Alpak, F.O., Dussan V., E.B., Habashy, T.M., and Torres-Verdín, C., 2003, "Numerical simulation of mud filtrate invasion in horizontal wells and sensitivity analysis of array induction tools," *Petrophysics*, v. 44, no. 6, pp. 396-411.

Archie, G.E., 1942, "The electrical resistivity log as and aid in determining some reservoir characteristics," *Petroleum Transactions, AIME*, v. 146, pp. 54-62.

Balan, B., Mohagheh, S., and Armeri, S., 1995, "State-of-the-art in permeability determination from well log data: Part 1- A comparative study, model development," paper SPE 30978 presented at the SPE Eastern Regional Conference and Exhibition, Morgantown, West Virginia, September 17-21, 10 p.

Bigelow, E., 1992, "*Introduction to Wireline Log Analysis*," Western Atlas International, Inc., Houston, TX.

Chew, W.C., Barone, S., Anderson, B., 1984, and Henessy, C, "Diffraction of axisymmetric waves in a borehole by bed boundary discontinuities," *Geophysics*, v. 49, no. 10, pp. 1586-1595.

Chew, W.C. and Liu, Q.H., 1994, "Inversion of induction tool measurements using the distorted Born iterative method and CG-FFHT," IEEE *Trans. Geosciences and Remote Sensing*, v. 32, no. 4, pp. 878-884.

Clavier, C., Coates, G. Dumanoir, J., 1984, "Theoretical and experimental bases for the dual-water model for interpretation of shaly-sands," *SPE Journal*, v. 24, no. 2 pp. 153-168.

Dewan, J.T., 1983, "*Essentials of Modern Open-Hole Log Interpretation*," PennWell Publishing Company, Tulsa, OK.

Doll, H.G., 1949, "The S.P. log: theoretical analysis and principles of interpretation," *Transactions AIME*, v. 179, pp. 146-185.

Habashy, T.M. and Abubakar, A., 2004, "A general framework for constrained minimization for the inversion of electromagnetic measurements," *Progress in Electromagnetic Research*, PIER 46, pp. 265-312.

Hallemburg, J.K., 1971, "A resume of spontaneous potential measurements," paper U presented at the 12th Annual Logging Symposium: Society of Professional Well Log Analysts, El Paso, TX, May 2-5, 16 p.

Luffel, D.L., Howard, W.E., and Hunt, E.R., 1991, "Travis Peak Core Permeability and Porosity Relationships at Reservoir Stress," *SPE Formation Evaluation*, v. 6, n. 3, pp. 310-318.

Pickett, G.R., 1966, "A review of current techniques for determination of water saturation from logs," *Journal of Petroleum Technology*, v. 18, no. 11, pp. 1425-1433.

Pirson, S.J., 1963, "*Handbook of Well Log Analysis: For Oil and Gas Formation Evaluation*," Prentice-Hall, Inc., Englewood Cliffs, NJ.

Salazar, J.M., Torres-Verdín, C., and Sigal, R., 2005, "Assessment of permeability from well logs based on core calibration and simulation of mud-filtrate invasion," *Petrophysics*, v. 46, no. 6, pp. 434-451.

Salazar, J.M., Torres-Verdín, C., Alpak, F.O., Habashy, T.M., and Klein, J.D., 2006, "Estimation of permeability from borehole array induction measurements: application to the petrophysical appraisal of tight-gas sands," *Petrophysics*, v. 47, no. 6, pp. 527-544.

Schlumberger, 1991, "*Log Interpretation Charts*," Schlumberger Educational Services, U.S.A.

Segesman, F., 1962, "New SP correction charts", *Geophysics*, v. 27, no. 6, pp. 815-828.

Wu, J, Torres-Verdín, C., Sepehrnoori, K., and Proett, M.A., 2005, "The influence of water-base mud properties and petrophysical parameters on mudcake growth, filtrate invasion, and formation pressure," *Petrophysics*, v. 46, no. 1, pp. 14-32.

Wyllie, M.R.J. and Southwick, P.F., 1954, "An experimental investigation of the S.P. and resistivity phenomena in dirty sands," *Journal of Petroleum Technology*, v. 6, no. 2, pp. 44-57.

Zhang, G.J., 1984, "*Electrical Logging*," Petroleum Industry Press, Beijing, China.

Zhang, G.J. and Wang, G.L., 1997, "Application of vector potential theory to spontaneous potential calculation," *Radio Science*, v. 32, no. 3, pp. 899-905.

Zhang, G.J. and Wang, G.L., 1999, "A new approach to SP-vector potential approach," *IEEE Transactions on Geoscience and Remote Sensing*, v. 37, no. 4, pp. 2092-2098.

Zhang, G.J., Wang, G.L., and Wang, H.M, 1999, "Application of novel basis functions in a hybrid method simulation of the response of induction logging in axisymmetrical stratified media," *Radio Science*, v. 34, no. 1, pp. 19-26.

APPENDIX A: FORWARD MODEL AND RESISTIVITY INVERSION

Forward Model: In this paper, we adopt a 2D axial-symmetric model. In such a model, current loop sources reside at the center of borehole with a magnetic moment pointing upward; the conductivity (σ) is invariant in the azimuthal direction. Sedimentary rocks are generally non-magnetic, hence the magnetic permeability (μ) is assumed equal to the vacuum magnetic permeability (μ_0). As a result, the electric field comprises only the azimuthal component (E_φ) and varies only in the meridian plane. Assuming that there is only one source current loop, with radial position r_s, and vertical position z_s, the governing equation is giving by

$$\left[\frac{\partial}{\partial r}\frac{1}{r}\frac{\partial}{\partial r}r+\frac{\partial^2}{\partial z^2}+\kappa^2\right]E_\varphi(r,z;r_s,z_s)= -i\omega\mu_0 I\delta(r-r_s)\delta(z-z_s), \quad \text{(A.1)}$$

where I is the electric-current intensity, δ is Dirac's delta function, ω is angular frequency, $\kappa^2 = i\omega\mu_0\sigma$, and $i = \sqrt{-1}$. The boundary condition is $E_\varphi(r,z)|_{\partial\Omega} = 0$, where $\Omega = \{(r,z) | 0 \le r < \infty, -\infty < z < \infty\}$.

We assume a piecewise-constant spatial distribution of electrical conductivity, i.e.,

$$\sigma(r,z) = \sigma_0(r)H(z_1 - z) + \sigma_M(r)H(z - z_M) + \sum_{m=1}^{M-1} \sigma_m(r)\left[H(z - z_m) - H(z - z_{m+1})\right], \quad \text{(A.2)}$$

where *H(z)* is the Heaviside function. There is a total of *M+1* horizontal layers with boundaries z_1, z_2, …, z_M, and layer conductivities given by

$$\sigma_m(r) = \sigma_{mud}H(r_w - r) + \sigma_{t,m}H(r - r_{inv}) + \sigma_{xo,m}(r)\left[H(r - r_w) - H(r - r_{inv})\right],$$

$m = 0,1,...,M$.

Therefore, layer conductivities are functions of the radial length of invasion (r_{inv}), borehole radius (r_w), borehole conductivity (σ_{mud}), and invaded- and virgin-zone conductivities (σ_{xo} and σ_t), respectively.

We make use of the Numerical-Mode Matching Method (NMM) to solve the above 2D simulation problem (Chew et al., 1984; Zhang et al., 1999). This algorithm combines a 1D finite element solution in the radial direction with an analytical solution in the vertical direction. When augmented by the new type of basis functions (Zhang et al., 1999), the NMM is several times more computer efficient than 2D finite-element and finite-difference methods.

Inversion: We minimize the quadratic cost function given by

$$C(\bar{\mathbf{x}}) = \frac{1}{2}\left\{\left\|\bar{\mathbf{e}}(\bar{\mathbf{x}})\right\|^2 + \lambda^2\left\|\bar{\mathbf{x}}\right\|^2\right\}, \quad \text{(A.3)}$$

where $\bar{\mathbf{x}}$ is the unknown model parameters (layer-by-layer values of R_{xo}, R_t, and r_{inv}), λ^2 is a regularization (stabilization) parameter, and $\bar{\mathbf{e}}$ is the vector of data residuals given by

$$\bar{\mathbf{e}}(\bar{\mathbf{x}}) = \bar{\mathbf{d}}_o(\bar{\mathbf{x}}) - \bar{\mathbf{d}}^o.$$

In the above expressions, $\bar{\mathbf{d}}_o(\bar{\mathbf{x}})$ contains the simulated measurements and $\bar{\mathbf{d}}^o$ contains the field measurements (raw AIT conductivities).

We approach the minimization of the cost function given by equation (A.3) using the distorted Born iterative method (DBIM) (Chew and Liu, 1994). The computation of sensitivities (entries of the Jacobian matrix) is crucial to the solution of the nonlinear minimization problem. We now proceed to show how we overcome this problem. Consider a generic single-transmitter single-receiver induction system. Let r_T be the radial location and z_T be the vertical location of the transmitter. Likewise, let r_R and z_R be the radial and vertical locations of the receiver, respectively. When applying a perturbation $\Delta\sigma$ to the background conductivity σ^0, the correspondent perturbation on apparent conductivity is given by

$$\Delta\sigma_a = \int_0^\infty\int_{-\infty}^\infty dr dz\; g(r,z)\Delta\sigma(r,z), \quad \text{(A.4)}$$

where

$$g(r,z) = \mathrm{Re}\left\{-\frac{2\pi\omega^2\mu_0^2 I}{\mathrm{K}} rG(r,z;r_R,z_R)G(r,z;r_T,z_T)\right\},$$ K is the tool constant, and $G(r,z;r_s,z_s)$ is the Green's function that satisfies equation (A.1) with the right-hand side replaced with $-\delta(r - r_s)\delta(z - z_s)$.

Substitution of equation (A.2) into equation (A.4) yields

$$\begin{aligned}
\frac{\partial\sigma_a(r,z)}{\partial\Delta\sigma_{i,m}} &= \int_{r_w}^{r_{i,m}}\int_{z_m}^{z_{m+1}} dr dz\; g(r,z) \\
\frac{\partial\sigma_a(r,z)}{\partial\Delta\sigma_{t,m}} &= \int_{r_w}^{\infty}\int_{z_m}^{z_{m+1}} dr dz\; g(r,z) \\
\frac{\partial\sigma_a(r,z)}{\partial r_{inv,m}} &= (\sigma_{i,m} - \sigma_{t,m})\int_{z_m}^{z_{m+1}} dz\; g(r_{i,m},z)
\end{aligned} \quad . \quad \text{(A.5)}$$

In the above equations, we assume that the formation boundary z_m is known. Initially in the DBIM, the Jacobian matrix, whose entries are given by equation (A.5), is re-calculated after updating the conductivity (Chew and Liu, 1994). Since the induction problem is quasi-linear (Zhang, 1984), the Green's function is approximated with that of a homogeneous medium penetrated by a borehole and fixed for all iteration steps. Consequently, at each step, the Jacobian matrix is reset by evaluating only the three integrals given by equation (A.5). This approach represents a highly cost-effective process because the evaluation of *g(r,z)* is not necessary. For the inversion, we assume that σ_{mud} and r_w are known and that the conductivity of the

H

homogeneous medium is equal to 0.001 S/m. The above strategy greatly reduces the computer cost required by the calculation of derivatives.

The multiplicative regularization technique (Habashy and Abubakar, 2004) allows us to calculate the regularization parameter with the relationship

$$\lambda^2 = \frac{\left\| \bar{\mathbf{e}}\left(\bar{\mathbf{x}}\right) \right\|^2}{\beta},$$

where β is a constant that can be determined with numerical experiments and in our case is equal to 2.0. In thick formations (over hundreds of feet long) containing many layers, the inversion process acts as a window sliding over the data set layer-by-layer. This is possible because induction is primarily a localized measurement, namely, the apparent conductivity is mostly affected by the media close to the measurement point whereas the effect of media far from the measurement point is comparatively small.

Results obtained from the inversion of resistivity for each layer (R_{xo}, R_T, and r_{inv}) are the main inputs for the inversion of SP measurements. The inversion of SP is posed as linear problem and we use the SVD method to solve the system of equations. Finally, we obtain the value of *SSP* at each layer boundary. The maximum *SSP* in absolute value is used to calculate connate water resistivity as previously explained in this paper.

ABOUT THE AUTHORS

Jesús M. Salazar is a Research Assistant and a Ph.D. Candidate in the Department of Petroleum and Geosystems Engineering of The University of Texas at Austin. He received a B.Sc. degree in Physics (with honors) from Universidad Central de Venezuela in 1998 and a M.Sc. degree in Petroleum Engineering from The University of Texas at Austin in 2004. From 1997 to 2002, he worked for PDVSA (Maracaibo, Venezuela) as a petrophysicist and well-log analyst. Jesús has also worked as a summer intern for ConocoPhillips and Occidental Oil and Gas Corporation performing petrophysical interpretation and modeling. He was bestowed a student grant, 2002-2003, and three scholarships, 2003-2004, 2005-2006, and 2006-2007 by the SPWLA. His research interests include petrophysics, log analysis, inverse problems, and numerical reservoir simulation.

Gong Li Wang received a B.Sc. degree in geophysical well logging and a Ph.D. degree in geophysics from the University of Petroleum, East China, in 1993 and 2001, respectively. From 1993 to 2002, he was affiliated with the University of Petroleum, East China teaching courses and conducting research on electromagnetic well logging. From 2002-2005, he was a Visiting Scholar and a Postdoctoral Research Associate with the Center for Computational Electromagnetics, University of Illinois at Urbana-Champaign. Since 2005, he has been a Postdoctoral Research Fellow and a Research Associate with the Center for Petroleum and Geosystems Engineering of The University of Texas at Austin. In 2001, he was awarded the Second Class Prize of the Award for Technological Innovation by China National Petroleum Corporation. His research interest is in wave propagation in inhomogeneous media, numerical modeling methods, and inverse problem.

Carlos Torres-Verdín received a Ph.D. degree in Engineering Geoscience from the University of California, Berkeley, in 1991. During 1991–1997 he held the position of Research Scientist with Schlumberger-Doll Research. From 1997–1999, he was Reservoir Specialist and Technology Champion with YPF (Buenos Aires, Argentina). Since 1999, he has been with the Department of Petroleum and Geosystems Engineering of The University of Texas at Austin, where he currently holds the position of Associate Professor. He conducts research on borehole geophysics, well logging, formation evaluation, and integrated reservoir characterization. Torres-Verdín has served as Guest Editor for Radio Science, and is currently a member of the Editorial Board of the Journal of Electromagnetic Waves and Applications, and an associate editor for Petrophysics (SPWLA) and the SPE Journal. He is co-recipient of the 2003 and 2004 Best Paper Award by Petrophysics, and is recipient of SPWLA's 2006 Distinguished Technical Achievement Award.

Hee Jae Lee is a Research Assistant and currently a Ph.D. candidate in the Department of Petroleum and Geosystems Engineering of The University of Texas at Austin. He is working in the Formation Evaluation Research Group supervised by Dr. Torres-Verdín. Hee-Jae has B.Sc. and M.Sc. degrees in Petroleum Engineering from Hanyang University, Korea. His main research area is in geomechanical-fluid flow coupling, and near wellbore simulation. He is the main code developer of the University of Texas, Formation Evaluation Tool Box (UTFET) and Formation Tester Toolbox (UTFTT).